

See discussions, stats, and author profiles for this publication at: <https://www.researchgate.net/publication/255820043>

Assessment of the attained temperatures and of melting in the nanosecond irradiation of doped poly (methylemethacrylate) at 308, 248, and 193

ARTICLE *in* JOURNAL OF APPLIED PHYSICS · OCTOBER 2005

Impact Factor: 2.18 · DOI: 10.1063/1.2076430

CITATIONS

9

READS

30

5 AUTHORS, INCLUDING:



Giannis Bounos

Foundation for Research and Technology - H...

26 PUBLICATIONS 219 CITATIONS

SEE PROFILE



Andreas Kolloch

11 PUBLICATIONS 71 CITATIONS

SEE PROFILE

Assessment of the attained temperatures and of melting in the nanosecond irradiation of doped poly(methylmethacrylate) at 308, 248, and 193nm via the examination of dopant reactivity

Giannis Bounos, Andreas Kolloch, Taxiarchos Stergiannakos, Erene Varatsikou, and Savas Georgiou

Citation: *J. Appl. Phys.* **98**, 084317 (2005); doi: 10.1063/1.2076430

View online: <http://dx.doi.org/10.1063/1.2076430>

View Table of Contents: <http://jap.aip.org/resource/1/JAPIAU/v98/i8>

Published by the American Institute of Physics.

Additional information on J. Appl. Phys.

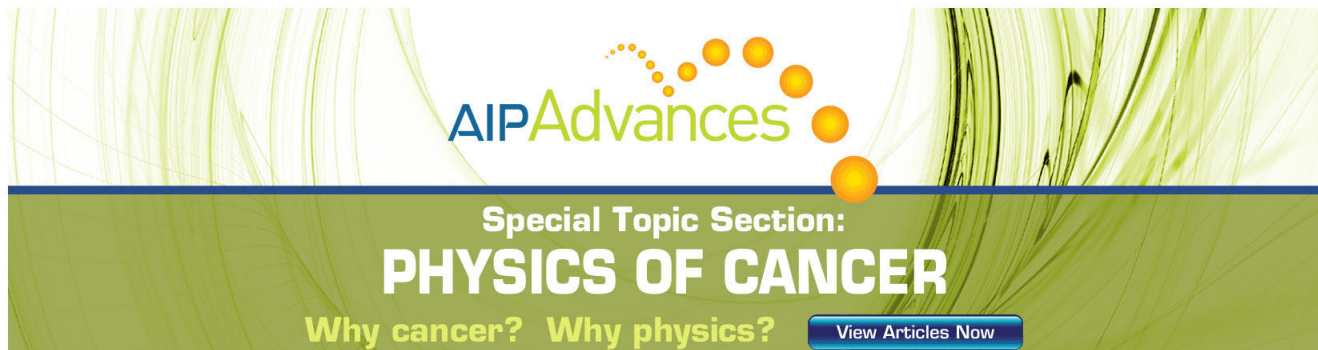
Journal Homepage: <http://jap.aip.org/>

Journal Information: http://jap.aip.org/about/about_the_journal

Top downloads: http://jap.aip.org/features/most_downloaded

Information for Authors: <http://jap.aip.org/authors>

ADVERTISEMENT

The advertisement features a green background with abstract, flowing white lines. In the center, the text 'AIPAdvances' is displayed in a green, sans-serif font, with a series of orange dots forming an arc above it. Below this, the text 'Special Topic Section:' is in a smaller font, followed by 'PHYSICS OF CANCER' in a large, bold, white font. At the bottom, the text 'Why cancer? Why physics?' is in a green font, and a blue button with the text 'View Articles Now' is on the right.

AIPAdvances

Special Topic Section:
PHYSICS OF CANCER

Why cancer? Why physics? [View Articles Now](#)

Assessment of the attained temperatures and of melting in the nanosecond irradiation of doped poly(methylmethacrylate) at 308, 248, and 193 nm via the examination of dopant reactivity

Giannis Bounos,^{a)} Andreas Kolloch,^{b)} Taxiarchos Stergiannakos,^{c)} Erene Varatsikou,^{c)} and Savas Georgiou^{d)}

Institute of Electronic Structure and Laser, Foundation for Research and Technology-Hellas, 71110 Heraklion, Crete, Greece

(Received 26 April 2005; accepted 24 August 2005; published online 28 October 2005)

The thermal and structural changes effected to poly(methylmethacrylate) (PMMA) upon irradiation at 308, 248, and 193 nm are assessed via the examination of the formation yields of the products formed by the photolysis of iodoaromatics (iodonaphthalene and iodophenanthrene–ArI–) dopants. Specifically, the main aryl product, the hydrogen-substituted derivative ArH, is formed via a thermally activated process (hydrogen-atom abstraction); thus, its formation efficiency reflects the temperature evolution in the substrate following UV irradiation. In the case of iodonaphthalene dopant, biaryl species (1,1-binaphthalene and perylene) are also formed via diffusion-limited reaction of the aryl radicals; thus, their yield reflects the extent of polymer melting. To this end, laser-induced fluorescence is employed for the quantification of the aryl products formed in the substrate as a function of the irradiation fluence. At all wavelengths, the ArH amount scales linearly with F_{laser} at low fluences, but at higher fluences, it increases sharply reaching a plateau near the ablation threshold. Only quantitative differences concerning the fluence onset of the ArH increase and the amount of product remaining in the substrate are observed. Simulations accounting for the temporal and spatial evolutions of the temperature reproduce well the observed F_{laser} dependences. The quantitative differences in the extent of ArH formation are well accounted by the extent of the heat diffusion to the sublayers. Thus, contrary to many previous suggestions, a thermal process is demonstrated to be dominant at the three wavelengths. Concerning the biaryl species, their yield decreases from 308 to 193 nm. The simulation of their formation yield provides semiquantitative information about the polymer viscosity changes (melting) upon irradiation at the three wavelengths. Besides the mechanistic implications, the study also provides insight into the factors affecting the extent of chemical modifications in laser processing of polymers and organic substrates in general. In particular, the reduced extent of chemical modifications upon ablation at strongly absorbed wavelengths is indicated to be crucial for the success of these procedures. © 2005 American Institute of Physics. [DOI: [10.1063/1.2076430](https://doi.org/10.1063/1.2076430)]

I. INTRODUCTION

UV ablation constitutes the basis for a wide range of powerful techniques aiming at the analysis and processing of molecular substrates (e.g., in microelectronics,^{1–7} biology and medicine,⁸ art conservation,⁹ etc). As a result of this importance, substantial effort has been directed towards the elucidation of the mechanisms responsible for the laser-induced material ejection process. To this end, a wide range of studies (e.g., summarized in Refs. 1–6) has been reported on the dependence of the phenomenon on laser irradiation and material parameters. Particular emphasis has been placed on the influence of laser wavelength, since the use of short wavelengths is often advocated to promote a photochemical mechanism at the expense of a thermal one.¹ According at

least to the “simplest” version of this mechanism, for irradiation at wavelengths absorbed by photolabile units (usually the case for excitation at short UV wavelengths), material ejection is due to the expulsion exerted by the high number of (translationally “hot”) photofragments and/or by the large number of (expanding) gaseous products. The operation of such a mechanism is considered^{1–5} to differentiate qualitatively UV laser ablation from the IR-induced one resulting in the minimization of the thermal “load” to the substrate and in a highly “improved”/smooth morphology of the processed area.

However, despite much effort, it has proved difficult to establish this differentiation of mechanisms.^{1–5,10–23} In many cases, different species are often observed for irradiation at different wavelengths.^{1–5,8} However, the effective absorption coefficient changes much with wavelength thereby resulting in different temperatures and degree of thermal decomposition. The interpretation of the results is further complicated by the fact that gas-phase diagnostics are usually employed. Since the ejected species may be substantially modified by secondary photofragmentations/reactions in the plume, their

^{a)}Also at the Department of Physics, University of Crete, Crete, Greece.

^{b)}Also at the Department of Physics, University of Konstanz, Konstanz, Germany.

^{c)}Also at the Department of Chemistry, University of Crete, Crete, Greece.

^{d)}Author to whom correspondence should be addressed; FAX: ++ 30 81 391318; electronic mail: sgeorgiu@iesl.forth.gr

correlation with specific mechanism(s) remains always open to criticism. As a result of these problems, the contribution, if any, of photochemical mechanism and the importance of wavelength remain the most controversial issue in the field of ablation of organic substrates.

We have demonstrated previously¹¹ the potential of using simple photosensitive organic compounds such as iodonaphthalene, iodophenanthrene (ArI), etc., dispersed within polymers for studying aspects of UV ablation. The species remaining in the substrate following irradiation are monitored so that the interpretation of the results is free from the complications plaguing gas-phase studies. Most importantly, the aryl product formation affords direct information about the processes induced in the substrate upon laser irradiation. Specifically, the aryl (Ar) radicals produced by ArI photolysis may abstract a hydrogen from the polymer to form ArH, i.e., via a (thermally) activated process. Therefore, the yield of ArH product reflects the temperature evolution in the substrate following irradiation. In addition, at least for the NapI dopant, biaryl species (1,1-binaphthalene–Nap₂– and perylene) are also detected. For the employed dopant concentrations, these species are formed via diffusion-limited reaction. Consequently, their formation affords a direct experimental probe of the extent of the substrate melting upon laser irradiation (in contrast to the usual approach in which laser-induced melting is largely inferred by indirect morphological examination).

Here, we employ this approach for examining the processes induced upon the irradiation of poly(methylmethacrylate) (PMMA) at the excimer laser wavelengths of 193, 248, and 308 nm. The UV ablation of PMMA has been examined extensively and a number of conflicting hypotheses, ranging from “pure” photothermal to photochemical and even combination of them, have been advanced (especially for irradiation at 193 nm).^{1–5,12–25} To this end, we examine the formation yields of ArH and biaryl species in the irradiation of PMMA doped with ArI. Their yield is examined as a function of laser fluence (F_{laser}) (from $\approx 25 \text{ mJ/cm}^2$ to well over the ablation thresholds) thereby assessing the thermal and structural changes (melting) in the polymer with increasing laser fluence.

Importantly, the F_{laser} dependence of ArH amount in the substrate is found to be qualitatively the same at the three wavelengths. Only quantitative differences are observed concerning the product amount and the onset fluence for enhanced product formation. The observed dependences are well accounted by a thermal model, with the differences reflecting the different extent of heat diffusion to the substrate. The model is further quantified by the observations on the formation of the biaryl species. Overall, the study reinforces previous suggestions for the dominant operation of a thermal mechanism for irradiation at 308 and 248 nm. In addition, it establishes the dominance of thermal mechanism at 193 nm despite the variety of mechanisms that have been advanced previously for irradiation at this wavelength.

Besides the mechanistic implications for the UV ablation of PMMA, the study provides direct insight into the factors affecting the extent of chemical effects in the laser process-

ing of molecular substrates (e.g., in laser restoration of painted artworks, laser processing of tissues, etc.)

II. EXPERIMENT

The iodoaromatic dopants (ArI) do not fluoresce, whereas the aryl products (ArH, Nap₂) are relatively “good” emitters.^{26–28} Thus, the aryl products that are formed/remain in the substrate upon laser irradiation can be characterized and quantified via laser-induced fluorescence (LIF). To this end, a typical “pump-probe” scheme is employed. “Pumping” at 308 nm is effected with the output of a Lambda Physik EMG201 and with the output of a Lambda-Physik LPX150 at 248 nm and at 193 nm. Product fluorescence is induced by excitation at 248 nm (the probe wavelength is chosen so that absorption by the polymer matrix is minimal). The probe F_{laser} is $\approx 5\text{--}10 \text{ mJ cm}^{-2}$ —low enough to ensure that photolysis by the probe beam is negligible. The pump- and probe-laser beams are focused perpendicularly and co-axially onto the sample via a quartz spherical lens (the pump beam to a rectangle of $\approx 6\text{--}10 \times 10^{-2} \text{ cm}^2$ and the probing beam to a somewhat smaller size within the irradiated area). In all cases, the presented data are recorded for a single “pump” laser pulse on virgin sample (area). Irradiation is performed in air. A long delay (seconds) between the pump and probe pulses ensures the quantitative reaction of the aryl radicals and formation of stable products. Indeed, within the signal-to-noise (S/N) ratio, the product fluorescence intensity remains constant for longer delay times.

The induced emission is collected by an optical fiber oriented nearly perpendicular to the sample at $\sim 1\text{--}2 \text{ cm}$ away from its surface (i.e., front-face excitation mode is employed). Cutoff filters ($<290 \text{ nm}$) are used to minimize the influence of the probe-laser scattered light. The emission is spectrally analyzed in a 0.20 m grating spectrograph (300 grooves/mm grating) and recorded on an optical multichannel analyzer (OMA III system, EG&G PARC Model 1406) interfaced to a computer. Synchronization of the two lasers and of the detector is effected by a digital pulse generator (Stanford). For the further characterization of the products, temporally resolved fluorescence spectra are recorded for various detection gates of the OMA.

Poly(methyl methacrylate) (Aldrich, average $M_w \sim 120 \text{ K}$) is subjected to extensive purification. The iodoaromatics (Aldrich) are purified by flash chromatography. 1,1-binaphthyl and perylene (Aldrich) are employed as received. Samples are prepared by casting solutions (in CH_2Cl_2) of the polymer and of the dopant on quartz plates. The samples are dried initially in air and then *in vacuo*. The film thickness is typically in the $10\text{--}30 \text{ }\mu\text{m}$ range, as measured by profilometer (Diftek).

The surface morphology of the irradiated substrates has been examined by profilometry. As commonly observed,^{1–8} for irradiation at weakly absorbed wavelengths, polymer swelling is induced over a fluence range below the ablation threshold. The onset of swelling and the etching thresholds for the examined systems are collected in Table I.

TABLE I. Data concerning the examined ArI/PMMA systems.

System (wt. %)	Wavelength (nm)	α_{small}^a (cm ⁻¹)	α_{eff}^a (cm ⁻¹)	Swelling onset ^b (mJ/cm ²)	Ablation threshold ^b (mJ/cm ²)
0.5% PhenI/PMMA	193	≈ 6000 (≈ 1500)	≈ 6000	...	100
	248	2000 (1860)	2750–3000	200	700
	308	70 (40)	600	1200	3500
0.4% NapI/PMMA	193	≈ 4500 (≈ 400)	≈ 4500	...	170
	248	210 (60)	1000–1300	700	1100
	308	60 (20)	300–500	1700	3500
1.2% NapI/PMMA	193	≈ 5500 (≈ 1200)	≈ 5500	...	130
	248	350 (190)	2000–2500	500	900
	308	100 (65)	700	1200	2500

^aAbsorption coefficients determined from measurements of films cast on suprasil substrates. The numbers within the brackets indicate the absorptivity due to the dopant, as determined from literature values.^{26–28} The absorption coefficients of the doped PMMA differed somewhat depending on the degree of polymer purification (e.g., at 248 nm, it is measured to be ≈ 80 – 200 cm⁻¹). [Literature values show an even higher scatter (50 cm⁻¹ up to ≈ 500 cm⁻¹). At 193 nm, our measurements are closer to the value reported by Srinivasan *et al.* (Ref. 15) (vs the 2000 cm⁻¹ reported by others).

^bSwelling onset and ablation thresholds by profilometric examination of the indicated samples *following irradiation with one laser pulse* (at 193 nm, it was difficult to characterize the swelling and thus no fluence values are reported).

III. RESULTS

The probe LIF spectra recorded following the irradiation of lightly doped ArI/PMMA (≤ 0.8 wt %) at the three wavelengths exhibit an emission band centered at ~ 330 nm in the case of NapI or at ~ 370 nm in the case of PhenI [Fig. 1(a)]. By comparison with the spectra recorded for NapH/PMMA (PhenH/PMMA) films, the band is ascribed^{26,28} to the $^1B_{3u} \rightarrow ^1A_{1g}$ transition characteristic of NapH (PhenH). In all cases, the decay lifetime of the emission (100 ± 25 ns at $\lambda = 332$ nm) is found to be in good correspondence with the NapH (PhenH) fluorescence lifetime. Thus, in all cases ArH is the main or exclusive product. (In the case of 248 nm irradiation of ArI/PMMA, this conclusion has also been confirmed by gas chromatography/mass spectrometric examination.) Indeed, hydrogen-atom abstraction is the exclusive mode of reaction for methylnaphthyl radicals with PMMA (in solution).^{29,30}

Upon the irradiation of NapI/PMMA with dopant concentrations > 1 wt % at high fluences, the probe spectra exhibit, in addition, a broadband around 360 nm and two peaks at 430 and 450 nm [Fig. 1(b)]. As shown before¹⁰ and confirmed by direct comparison with spectra recorded from PMMA doped with the authentic compounds, the band at 360 nm is ascribed to 1,1-binaphthalene (Nap₂) and the double peak structure to perylene (this represents the fusion of two naphthalene systems).²⁸ For the PhenI dopant, Phen₂ formation cannot be ascertained, because Phen₂ fluorescence is not well differentiated from that of PhenH.

For the quantitative characterization of the ArH product, the probe fluorescence intensity (at $\lambda = 332$ nm–NapH–or $\lambda = 370$ nm–PhenH–) is plotted as a function of the pump laser fluence (Fig. 2). For the examined dopant concentrations (≤ 2 wt %) and film thickness (10–20 μm), the films are approximately optically thin (absorbance ≈ 0.3 – 0.4) at the probing wavelength. Thus, at low pump fluences, the fluorescence intensity is directly proportional to the amount of the aromatic product in the substrate (i.e., minimal self-absorption effects). However, at higher fluences, the induced modified film morphology results in enhanced scattering of the probe beam, so that the fluorescence intensity may not represent accurately the product amount in the substrate. Comparative examination with systems doped with photo-stable compounds (CdSe quantum dots) indicates the discrepancy to be 10%–15%. The differences observed between the systems are significantly larger than this, so that this deviation is of no particular consequence.

Most importantly at the three examined excimer wavelengths, the F_{laser} dependence of the ArH product is found to be qualitatively similar (Fig. 2). At low fluences, the product intensity scales linearly with the pump F_{laser} (slope in log-log plots generally 1.0 ± 0.2 , as determined from five or six measurements on each system) consistent with a one-photon dissociation of the dopants. Calibration/comparison with fluorescence measurements on ArH-doped PMMA³¹ shows that at these fluences, less than 10% of the photoexcited dopant reacts to ArH. However, at higher fluences, the ArH amount

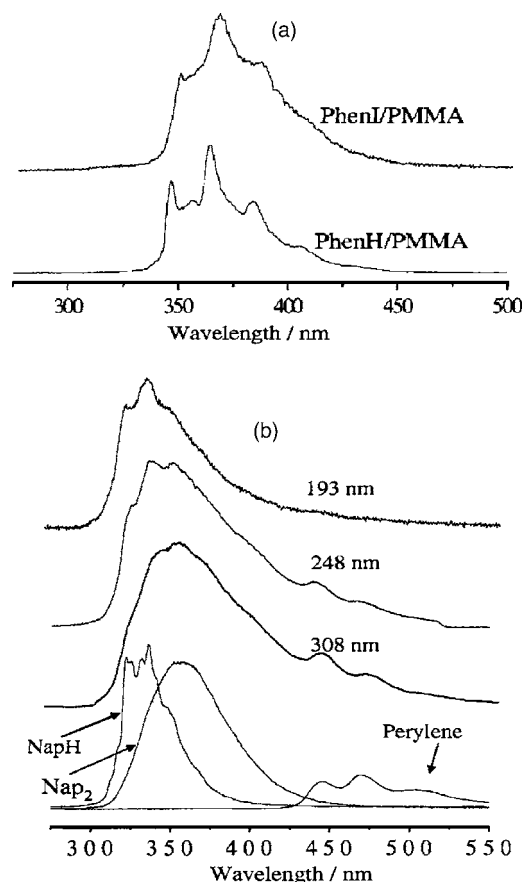


FIG. 1. (a) Probe product LIF spectra following irradiation with one 248 nm laser pulse of PhenI/PMMA (0.5 wt %). Spectrally identical product spectra are recorded following irradiation at any excimer wavelength. For comparison purposes, a spectrum recorded from PhenH/PMMA is also illustrated. (b) Probe product LIF spectra recorded from 1.2 wt % NapI/PMMA following irradiation at 308, 248, and 193 nm (in all cases probing effected at 248 nm) at fluences close to the corresponding ablation thresholds (Table I). For comparison purposes, the LIF spectra recorded from PMMA doped with the indicated compounds are also depicted.

grows sharply with increasing F_{laser} . The onset fluence for this deviation is observed to scale roughly inversely with the effective absorption coefficient α_{eff} of the systems (Table I).

Product intensity reaches a plateau at fluences close to the ablation thresholds of the systems. Examination of the plasma emission induced by the pump pulse, as well as transmission measurements of the pump laser beam, shows that shielding (i.e., absorption of the pump beam by the plume)³² becomes important at fluences somewhat higher than the corresponding ablation thresholds. Thus, the leveling off of the ArH product must be ascribed to the etching process. Importantly, for a given polymer/dopant, the signal at the plateau (i.e., the quantity of ArH product remaining upon ablation) at weakly absorbed wavelengths is quite higher than that at strongly absorbed ones (even for optically thin films).

It is clear that notwithstanding chemical characteristics of the employed dopants and polymers, the quantitative features of the F_{laser} dependence of the ArH product are mainly determined by the absorptivity of the dopant/polymer substrate. To illustrate further this feature, we have examined the F_{laser} dependence for the 248 nm irradiation of PMMA doped with different dopant (PhenI) concentrations, i.e., different

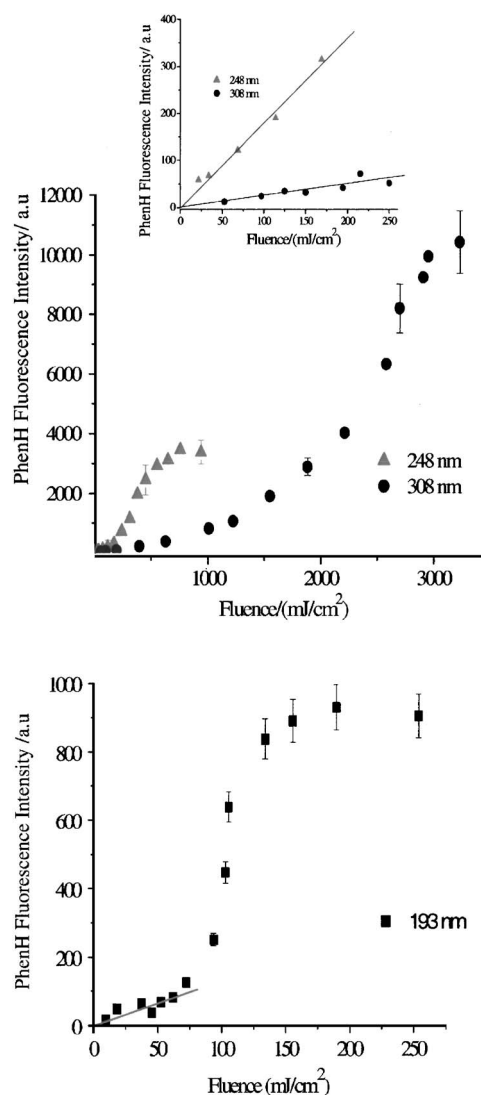


FIG. 2. F_{laser} dependence of the PhenH product in the irradiation of PhenI/PMMA (0.5 wt %) at (a) 308, 248, and (b) 193 nm (film thickness of $\approx 10 \mu\text{m}$). The error bars represent 2σ , as determined from at least five different measurements. In all cases, the fluorescence is recorded following irradiation with a single pump pulse. The inset illustrates the linear dependence observed for PhenH formation in the irradiation at very low laser fluences.

substrate absorptivities (Fig. 3). Qualitatively, the same dependence is observed for dopant concentrations as low as possible to permit reliable signal detection (~ 0.1 wt % PhenI). For a given dopant/polymer system, the onset of enhanced ArH formation decreases with increasing dopant concentration, i.e., increasing absorptivity. In parallel, the amount of product remaining in the substrate following ablation is much reduced despite the considerably higher number of photolabile chromophores present. Clearly, this result has direct and important implications for the laser processing of molecular substrates.

Concerning the biaryl species, for irradiation at the weakly absorbed 248 and 308 nm, these products are first detected for NapI concentrations of 0.8–1.2 wt % at fluences close to the onset of polymer swelling (Table I). With increasing pump-laser fluence, their yields grow until reaching a limiting value at the ablation threshold (Fig. 4). The emis-

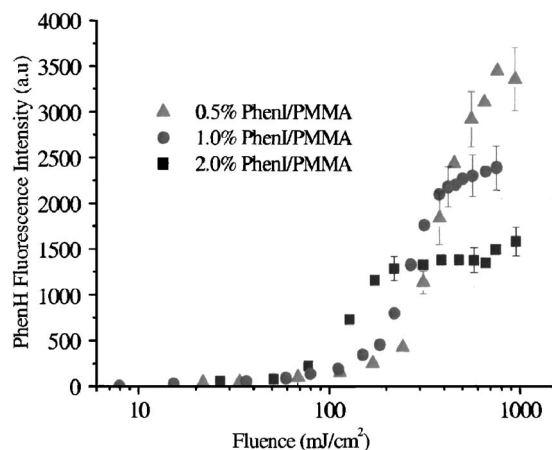


FIG. 3. F_{laser} dependence of PhenH product formed in the 248 nm irradiation of PMMA doped with 0.5, 1, and 2 wt % PhenI.

sion intensity of 1,1-binaphthalene (as well as of perylene—not shown)—measured at ≈ 380 nm at which the overlap by NapH emission is small—reaches higher values for irradiation at 308 nm than at 248 nm, whereas hardly any biaryl species emission is detected upon the 193 nm irradiation of the same dopant concentration.

IV. DISCUSSION

The present work has demonstrated that the dopant-deriving product patterns in the irradiation of iodoaromatics-doped PMMA at the three excimer laser wavelengths of 308, 248, and 193 nm follow well-defined trends:

- (1) The F_{laser} dependence of ArH formation is qualitatively the same for all systems, with the quantitative differences correlated with the substrate absorptivity at the irradiation wavelength.
- (2) For higher NapI concentrations (0.8–1.2 wt %), biaryl species (Nap₂ and perylene) are also detected, with the extent of their formation decreasing from 308 to 193 nm (evidently, in correspondence with increasing dopant/polymer absorptivity).

For accounting for these observations, we establish first the reaction(s) responsible for the formation of ArH and bi-

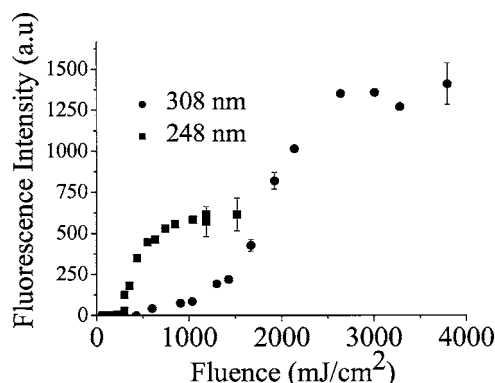


FIG. 4. Intensities of Nap₂ as a function of F_{laser} in the irradiation of 1.2 wt % NapI/PMMA at 248 and 308 nm. The error bars indicate the likely error in the estimation of the Nap₂ via the deconvolution procedure.

aryl products. Given the 2.6 eV energy of C–I bond,^{10,26,27} thermal decomposition of ArI can be discounted (less than 10^{-3} of ArI is estimated to decompose thermally even if temperatures as high as 2000 K are attained in the nonejected layers). At the three examined wavelengths, ArI absorb moderately or strongly²⁸ dissociating into Ar and I radicals with a quantum yield of ≈ 1 upon excitation.²⁷ Due to the very fast photodissociation of ArI (≈ 1 ps),²⁷ product formation via direct reactions of excited states can be ruled out. Therefore, the aryl products are formed exclusively by reactions of aryl (Ar) radicals formed by the ArI photodissociation. Based on the known chemistry of aryl radicals, the ArH product is formed by hydrogen-atom abstraction from the polymer and the biaryl species by diffusion-limited reaction(s) (Nap + Nap \rightarrow Nap₂).

In view of this conclusion, two factors have to be taken into account for modeling quantitatively product formation at the three wavelengths: (a) differences in the absorption step, thus resulting in different number and spatial distribution of the aryl radicals ($[\text{Ar}]$) and (b) changes in the subsequent reactivity of the photogenerated aryl radicals as a result of the different temperature and/or viscosity evolution in the irradiated substrates.

Concerning (a), absorption by ArI at low fluences is a one-photon process, as shown by the linear F_{laser} dependence of the ArH emission (inset in Fig. 2). However, even at higher fluences, ArI dissociation must proceed via one-photon excitation. Indeed, assuming an absorption cross section for the secondary step equal to that for C₆H₆ and related compounds,²⁸ fluences in excess of 5 J/cm² are required for a two-photon process to compete with the fast dissociation of ArI (the one-photon nature of ArI fragmentation at these fluences cannot be ascertained by transmission measurements of the pump pulse because of “competing” absorption by intermediates/polymer species, such as multiphoton processes, etc.)

However, besides absorption by ArI, what matters for the quantitative modeling/description is the effective absorption of the polymer/dopant system. This differs much at different wavelengths and even at a single wavelength with increasing F_{laser} . Indeed, at the weakly absorbed wavelengths (where ablation is effected at high fluences), transmission measurements of the pump beam show multiphoton processes to become significant at fluences well below the ablation thresholds. This agrees well with previous observations on related systems.^{19,33,34} Evidently, the aryl radicals formed by ArX photolysis and/or species of the polymer decomposition absorb additional photons. On the other hand, for irradiation at 193 nm, there is no clear evidence for a change (either multiphoton or saturation³⁵) in transmission measurements at fluences below the threshold. Clearly, the increase in ArH formation that is observed below the threshold is not due to absorption saturation effects (of the pump laser beam); instead, it represents an increase in the product amount formed per unit volume.

In view of the previous discussion, the observed dependence of ArH formation must reflect the dynamics of product formation. ArH formation can be described by a pseudomolecular hydrogen-atom abstraction by the Ar radicals [i.e.,

$d[\text{ArH}]/dt = A \exp[-E_{\text{act}}/RT(z, t)][\text{Ar}]$, where $[\text{Ar}]$ is the concentration of aryl radicals. Such reactions for small aromatic compounds are characterized by an activation energy E_{act} in the 40–60 kJ/mol range and a preexponential factor A of 10^5 – 10^7 s $^{-1}$.³⁶ For modeling the ArH formation, the temperature evolution in the substrate following irradiation is estimated by^{37,38}

$$T(z, t) = T_0 + \frac{\alpha_{\text{eff}} F_{\text{laser}}}{2C_p} \exp(\alpha_{\text{eff}}^2 D_{\text{th}} t) \times \left[\exp(-\alpha_{\text{eff}} z) \left(\alpha_{\text{eff}} \sqrt{D_{\text{th}} t} - \frac{z}{2\sqrt{D_{\text{th}} t}} \right) + \exp(\alpha_{\text{eff}} z) \text{erfc} \left(\alpha_{\text{eff}} \sqrt{D_{\text{th}} t} + \frac{z}{2\sqrt{D_{\text{th}} t}} \right) \right], \quad (1)$$

where z is the depth from the film surface (erfc: complementary error function). The formula neglects energy removal by desorption of volatile species (subablative regime) or by material ejection (ablation) as well as heat losses due to polymer decomposition. Nevertheless, it is a relatively good description of the temperature evolution below the ablation threshold over the microsecond-millisecond time scale that product formation takes place (as demonstrated by kinetic study,³⁹ product formation in the irradiation of ArI/PMMA is completed in ~ 600 μ s at 193 nm and at ~ 5 ms at 248 nm). $T_0 = 300$ K and for PMMA, $\rho = 1.19 \times 10^3$ kg m $^{-3}$, $C_p = 2 \times 10^3$ J kg $^{-1}$ K $^{-1}$ (25–250 °C) growing to $\approx 3 \times 10^3$ J kg $^{-1}$ K $^{-1}$ at higher temperatures and $D_{\text{th}} = 4 \times 10^{-8}$ m 2 s $^{-1}$.^{4,40} The effective absorption coefficients α_{eff} are fixed to *average* values determined by transmission measurements at selected pump-laser fluences below the thresholds (Table I) (whereas, the spatial distribution of Ar radicals is estimated via the absorption values for ArI). For the simulation, the substrate is divided in slabs and product formation is integrated over time.

Despite any uncertainties in the effective absorption coefficients and in the reaction rate constants, the simulation reproduces nearly quantitatively the F_{laser} dependence of the ArH product formation at the three wavelengths (for $E_{\text{act}} \approx 55$ kJ/mol) [Fig. 5(a)]. At low laser fluences, only a small percentage of the photoproducted Ar radicals react to ArH (the nonreacted radicals likely recombine eventually with the corresponding geminate halogen radical). With increasing laser fluence, the reaction efficiency increases sharply and in parallel, a higher percentage of the radicals in the sublayers reacts as a result of heat diffusion. Therefore, the reaction should be limited by the heat relaxation time $\tau_{\text{th}} = 1/(\alpha_{\text{eff}}^2 D_{\text{th}})$ ($\approx 10^{-3}$ – 10^{-2} s for the weakly absorbing and $\approx 10^{-5}$ – 10^{-4} s for the strongly absorbing systems). Accordingly, ArH formation should become important (i.e., reaction of fraction r of the photoproducted radicals) at $F_{\text{laser}} \approx (\rho C_p / \alpha_{\text{eff}}) \{ (E_{\text{act}}/R) / [\ln(A/a_{\text{eff}}^2 D_{\text{th}}) \ln(1/r)] - T_0 \}$. The estimated fluences (for $r \geq 0.13$) are found to be in good accord with the experimental F_{laser} values for the onset of enhanced ArH formation. Accordingly, the effective “reaction depth” can be approximated:

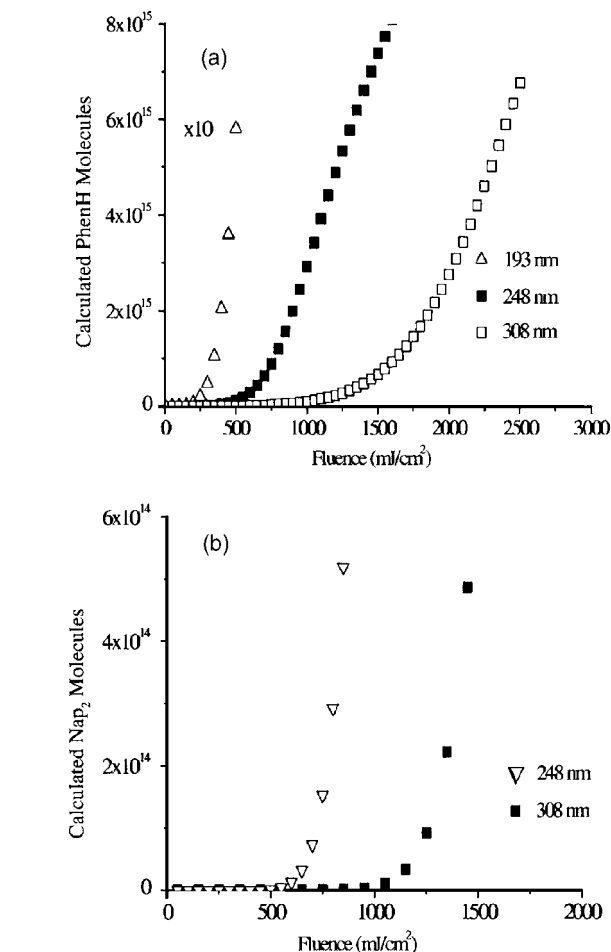


FIG. 5. (a) PhenH product estimated to form as a function of laser fluence in the irradiation of 0.5 wt % PhenI/PMMA at 308, 248, and 193 nm (film thickness=20 μ m). The details of the simulation are described in the text. (b) Estimated F_{laser} dependence of Nap₂ formation for irradiation of 1.2% NapI/PMMA at 308 and 248 nm (film thickness=20 μ m).

$$A \exp[-E_{\text{act}}/RT(z, t)] \times \tau_{\text{th}} \sim 1 \Rightarrow l_{\text{rxn}} = \sqrt{\frac{1}{\alpha_{\text{eff}}^2} \ln \left[\frac{(\alpha_{\text{eff}} F_{\text{laser}} / \rho C_p) [\ln A - \ln(\alpha_{\text{eff}}^2 D_{\text{th}})]}{(E_{\text{act}}/R)} \right]} \approx 7 - 10 \mu\text{m}$$

for weakly absorbing systems and ≈ 1 μ m for the strongly absorbing ones. Therefore, for the same absorbed energy $\alpha_{\text{eff}} F_{\text{laser}}$, the ArH yield decreases with increasing α_{eff} (assuming all other factors being the same), as experimentally demonstrated by the comparison of ArH formation in the irradiation of different dopant concentrations (Fig. 3).

Close to the ablation threshold, Eq. (1) fails. At these fluences, energy removal by material ejection and the sharp increase of the polymer C_p (due to the decomposition into smaller fragments) limit the attained temperatures thereby resulting in the observed leveling off of product formation in the remaining substrate (Figs. 2 and 3). The observation of a plateau is in accordance with the “blow-off” model: $l_{\text{ejected}} = 1/\alpha_{\text{eff}} \ln(F_{\text{laser}}/F_{\text{thr}})$, for $F_{\text{laser}} \geq F_{\text{thr}}$, where l_{ejected} represents the etching depth. According to this, the remaining substrate is subject to F_{thr} , with the additional radicals/products formed with increasing F_{laser} been removed by the etching process. (Of course, the formula does not provide any insight

for the dependence below the threshold and may fail quantitatively due to the neglect of heat diffusion.⁴¹⁾

In all, the modeling directly demonstrates that at the three excimer wavelengths, high enough temperatures are attained well below the threshold, consistent with a thermal mechanism. The estimated maximum surface temperatures at fluences close to the thresholds are $T \approx 900$ K at 308 and 248 nm (which corresponds well to previous assessments^{19,40)} and $T \approx 600$ K at 193 nm. Quantitative differences at the three excimer wavelengths are satisfactorily accounted by the different extent of heat diffusion. In particular, the contribution of a photochemical mechanism must be small enough. Otherwise, since multiphoton excitation/dissociation for ArI is unlikely, the ArH yield would scale linear at fluences below the ablation threshold, at sharp variance with the observed F_{laser} dependence (Figs. 2 and 3). However, though the correspondence between the simulation and experimental curves is very good at 308 and 248 nm, it is much less satisfactory for 193 nm (e.g., onset of enhanced ArH formation is observed at lower fluences than calculated). It has often been noted⁴ that thermal models have difficulties in the quantitative description of the 193 nm ablation of polymers including PMMA. For instance, the ablation threshold is lower than expected by photothermal decomposition, the deviation being ascribed either to the operation of photochemical processes or even to the influence of stresses. However, these explanations cannot account for the deviation in ArH formation at 193 nm (the comparison of the simulated curve in Fig. 5(a) with Fig. 2 shows that the deviation indicates *higher temperatures* than estimated by Eq. (1))

One possible explanation for this deviation may be that the heat released by exothermic reactions of polymer species/fragments produced upon irradiation at 193 nm contributes to the heating of the substrate. In recent molecular-dynamics simulations, Yingling and Garrison⁴² have suggested that this may be a significant aspect in the laser irradiation of photolabile/reactive systems (such a contribution was considered⁴² to be part of a “photochemical” mechanism, but this seems to be largely semantics. The important point is that high-temperature elevations are induced in any case.) On the other hand, the relatively good simulation of ArH formation at the 308 and 248 nm attained with the experimentally determined α_{eff} suggests that at these wavelengths, this contribution is not substantial (or, at least, it is compensated by the endothermic contribution of bond scission/decomposition processes). Though this seems to be an “attractive” explanation, the accuracy of modeling is not sufficient for the definite demonstration of this possibility (e.g., somewhat uncertain kinetic parameters as well as difficulty in establishing accurately the absorption coefficients at 193 nm).

Further information is obtained from the examination of the biaryl species formation. As demonstrated previously by a number of spectroscopic examinations, at the employed NapI concentrations (≤ 1.2 wt %), dopant aggregation is insignificant.¹⁰ Thus, Nap₂ and perylene must form exclusively via diffusion-limited reaction(s):



At the employed concentrations, the average distance between dopant molecules is ≈ 4 nm. Assuming Fickian-type diffusion,⁴³ the Nap diffusion length scales as $(6D_{\text{sp}}t)^{1/2}$, with $D_{\text{sp}} = k_B T / (6\pi\eta R_{\text{Nap}})$ (where k_B is the Boltzmann constant, η is the medium viscosity, and R_{Nap} is the naphthalene radius 3.4 Å). For Nap₂ formation on millisecond time scale (experimentally confirmed³⁹ by the kinetic study) and assuming for this interval an average temperature of ~ 600 K (as indicated by the ArH simulation), η for irradiation at 308 and 248 nm close to the corresponding ablation thresholds is estimated to be $\approx 10^2 - 10^3$ Pa s, comparable to the viscosity reported for polymer melts⁴³⁻⁴⁶ (on the other hand, the minimal detection of Nap₂ for 0.4 wt % NapI indicates a lower bound of $\approx 10^1$ Pa s).

We have modeled the Nap₂ formation in detail by a second-order reaction, with a Smoluchowski-type rate constant $K = 8k_B T / 300\eta$ (η : Pa s). At temperatures above the glass transition, the temperature dependence of polymer viscosity η is usually approximated by

$$\eta = \eta_0 \exp \left[\frac{-C_1(T - T_{\text{ref}})}{C_2 + (T - T_{\text{ref}})} \right]. \quad (2)$$

For PMMA, a number of somewhat different constants have been reported for this equation.⁴³⁻⁴⁵ Adjusted for the molecular weight employed here, the parameters adopted for the simulation are $T_{\text{ref}} \approx 433$ K, $\eta_0 \approx 3 \times 10^7$ Pa s, $C_1 \approx 8.86$, and $C_2 \approx 102$ K. T is estimated via Eq. (1). The influence of the competing H-abstraction reaction for ArH formation is taken into account as described above.

The simulation reproduces, at least semiquantitatively, the observed F_{laser} dependence of Nap₂ formation [Fig. 5(b)]. With increasing F_{laser} the Nap concentration increases and in addition, viscosity decreases further, so that a much higher percentage of radicals reacts to Nap₂. In considering next Nap₂ formation at the three UV wavelengths, two factors have to be taken into account: First, since the formation rate of biaryls scales as $[\text{Nap}]^2$ (i.e., on the number of photolyzed NapI molecules per unit volume), their yield decreases with increasing polymer absorptivity. This factor accounts partly for the reduced biaryl species formation at 193 nm (based on the relative absorption coefficient of NapI versus effective absorption coefficient, the concentration of dissociated NapI at 193 nm is estimated to be ≈ 3 times lower than at 248 nm, at the corresponding ablation thresholds). Second, the melt depth (approximately $\eta \leq 10^5$ Pa s) scales as⁴⁷ $h_{\text{melt}} \approx (1/\alpha_{\text{eff}}) \ln[\alpha_{\text{eff}} F_{\text{laser}} / \rho C_p (T_m - T_0)]$, for $F_{\text{laser}} > (T_m - T_0) \rho C_p / \alpha$ (T_m = melting temperature, T_0 = ambient temperature) (in fact, it also depends on heat diffusion and any material and energy desorption/removal). The nearly inverse dependence of h_{melt} on α_{eff} and the longer melt condition promote Nap₂ formation for the lower α_{eff} . This may account for the somewhat higher Nap₂ at 308 nm than at 248 nm, even though the NapI absorption coefficient at 308 nm is smaller (i.e., lower Nap concentration produced). In all, the thermal model consistently accounts for the extent of Nap₂ formation at 248 and 308 nm and for the failure to detect Nap₂ formation at 193 nm. Evidently, as compared to mor-

phological or even the more elaborate interferometric method.^{47,48} Nap₂ formation provides a highly sensitive probe of the polymer viscosity changes upon laser irradiation.

Despite the semiquantitative agreement, likely limitations of using Eq. (2) to model the viscosity of PMMA upon laser irradiation must be noted. In particular, the parameters in Eq. (2) derive from viscosity measurements at much lower temperatures than those attained upon laser irradiation. Furthermore, Eq. (2) neglects the fact that upon laser irradiation, polymer viscosity is, in parallel, affected by the polymer thermal decomposition, formation of gaseous bubbles, etc., within the substrate. This question is addressed through the examination of the kinetics of Nap₂ formation.³⁹

V. CONCLUSIONS AND IMPLICATIONS

We have examined the fluence dependence of ArH and biaryl species formation in the irradiation of ArI-doped PMMA at 308, 248, and 193 nm. As shown, the formation of these products provides a direct probe of the thermal and structural changes (i.e., melting) induced to the polymers upon irradiation. At all three wavelengths, the ArH product formation exhibits qualitatively the same F_{laser} dependence, with quantitative features being mainly specified by the substrate dopant/polymer absorptivity. The observed ArH dependence unambiguously establishes that high enough temperatures are attained at the three wavelengths. Further information about the induced viscosity changes upon laser irradiation derives from the examination of Nap₂ formation. In all, the results appear to be in accord with the “bulk photothermal model,”⁶ although as indicated in Sec. IV, subtler aspects of the processes do not seem to be still well described.

With respect to the previous conclusion, it is noted that in a number of studies on polymers doped with photolabile dopants (e.g., C₆H₅Cl, triazene, etc.), the possibility of a photochemical mechanism has often been suggested. For these dopants, decomposition results mainly in gaseous products (eg. HCl, Cl₂, CO, N₂, etc), unlike the products formed by the employed here ArI dopants. Thus, our findings do not exclude the possibility of a photochemical mechanism for systems with such dopants (especially if used at high concentrations).

Besides the mechanistic conclusions, the results have also important implications for laser processing applications of molecular substrates. In applications, irradiation at relatively strongly absorbed wavelengths is, generally, selected for ensuring efficient etching and good surface morphology.^{1–5,8,9} These are usually the only criteria employed for the selection of the optimal wavelength. However, according to the present work, strong absorption also results in the high reduction of (deleterious) chemical modifications in the substrate (e.g., reduced product of thermally activated reactions and in parallel, much reduced formation of recombination/diffusion by-products). Thus, besides the improved etching efficiency and substrate morphology, an additional reason for the importance of processing at strongly absorbed wavelengths relates to the high degree of “chemical

protection” afforded to processed molecular substrates (e.g., photorefractive keratectomy at 193 nm versus at other wavelengths, laser restoration of painted artworks at the strongly absorbed 248 and 193 nm versus at the weaker 308 nm). In practice, the applications (e.g., medicine-photorefractive keratectomy,⁸ laser restoration of painted artworks⁹) exploit the fact that the processed substrates have a multilayer structure, with the highly pigmented labile substrate being covered by layers which are highly absorptive and relatively chemically inert. This further ensures that deleterious chemical modifications to the sensitive underlayers are reduced.

ACKNOWLEDGMENTS

The work was supported by the Large Installations Plan DGXII (Project No. G/89100086/GEP) and by the TMR Programme (No. ERB FMRX-CT98-0188) and PENED 01EΔ419 administered by the Greek Ministry of Development. We thank Prof. P. Leiderer for his support of A.K. exchange to FORTH.

¹R. Srinivasan and B. Braren, *Chem. Rev. (Washington, D.C.)* **89**, 1303 (1989).

²*Photochemical Processing of Electronic Materials*, edited by I. A. Boyd (Academic, London, 1992).

³*Laser Ablation: Principles and Applications*, Springer Series in Material Science Vol. 28, edited by J. C. Miller (Springer, Berlin, 1994).

⁴D. Bäuerle, *Laser Processing and Chemistry*, (Springer, Berlin, 2000).

⁵T. Lippert and J. T. Dickinson, *Chem. Rev. (Washington, D.C.)* **103**, 453 (2003); T. Lippert, A. Yabe, and A. Wokaun, *Adv. Mater. (Weinheim, Ger.)* **105**, 9 (1997).

⁶N. Bityurin, B. S. Luk'yanchuk, M. H. Hong, and C. T. Chong, *Chem. Rev. (Washington, D.C.)* **103**, 519 (2003).

⁷S. Georgiou and F. Hillenkamp, *Chem. Rev. (Washington, D.C.)* **103**, 317 (2003).

⁸A. Vogel and V. Venugopalan, *Chem. Rev. (Washington, D.C.)* **103**, 577 (2003).

⁹S. Georgiou, V. Zafiropoulos, D. Anglos, C. Balas, V. Tornari, and C. Fotakis, *Appl. Surf. Sci.* **127–129**, 738 (1998); M. Lasithiotaki, A. Athanassiou, D. Anglos, S. Georgiou, and C. Fotakis, *Appl. Phys. A* **69**, 363 (1999).

¹⁰G. Paltauf and P. E. Dyer, *Chem. Rev. (Washington, D.C.)* **103**, 487 (2003).

¹¹G. Bounos, A. Athanassiou, D. Anglos, S. Georgiou, and C. Fotakis, *J. Phys. Chem.* **108**, 7052 (2004); A. Athanassiou, M. Lassithiotaki, D. Anglos, S. Georgiou, and C. Fotakis, *Appl. Surf. Sci.* **154/155**, 89 (2000); A. Athanassiou, E. Andreou, D. Fragouli, D. Anglos, S. Georgiou, and C. Fotakis, *J. Photochem. Photobiol., A* **145**, 229 (2001).

¹²R. J. Lade, I. W. Morley, P. W. May, K. N. Rosser, and M. N. R. Ashfold, *Diamond Relat. Mater.* **8**, 1654 (1999).

¹³S. Nishio and H. Sato, *Electr. Eng. Jpn.* **125**, 19 (1998).

¹⁴R. Larciprete and M. Stuke, *Appl. Phys. B* **42**, 181 (1987).

¹⁵R. Srinivasan, B. Braren, and K. G. Casey, *Pure Appl. Chem.* **62**, 1581 (1990).

¹⁶B. R. Arnold and J. C. Scaiano, *Macromolecules* **25**, 182 (1992).

¹⁷D. E. Hare and D. D. Dlott, *Appl. Phys. Lett.* **64**, 715 (1994).

¹⁸M. Tsunewaka, S. Nishio, and H. Sato, *Jpn. J. Appl. Phys., Part 1* **34**, 218 (1995).

¹⁹H. Furutani, H. Fukumura, and H. Masuhara, *J. Phys. Chem.* **100**, 6871 (1996); T. Masubuchi, H. Furutani, H. Fukumura, and H. Masuhara, *J. Phys. Chem. B* **105**, 2518 (2001); H. Fukumura, E. Takasashi, and H. Masuhara, *J. Phys. Chem.* **99**, 750 (1995), and references therein.

²⁰D. J. Krajnovich, *J. Phys. Chem. A* **101**, 2033 (1997).

²¹T. Lippert, R. L. Webb, S. C. Langford, and J. T. Dickinson, *J. Appl. Phys.* **85**, 1838 (1999).

²²H. Schmidt, J. Ihlemann, B. Wolff-Rottke, K. Luther, and J. Troe, *J. Appl. Phys.* **83**, 5458 (1998).

²³G. C. Blanchet, P. Cotts, and C. R. Fincher, *J. Appl. Phys.* **88**, 2975 (2000).

²⁴B. Hopp, M. Csete, K. Révész, J. Vinkó, and Zs. Bor, *Appl. Surf. Sci.*

- 96–98**, 611 (1996).
- ²⁵F. Wagner and P. Hoffmann, Appl. Phys. A **69**, S841 (1999).
- ²⁶E. Haselbach, Y. Rohner, and P. Suppan, Helv. Chim. Acta **73**, 1644 (1990).
- ²⁷M. Dzvonik, S. Yang, and R. J. Bersohn, J. Chem. Phys. **61**, 4408 (1974).
- ²⁸J. B. Birks, *Photophysics of Aromatic Molecules* (Wiley, London, 1970), p. 232.
- ²⁹S. Holdcroft and B. Z. Tang, J. Chem. Soc., Chem. Commun. **1991**, 280; B.-Z. Tang, S. S. Holdcroft, and J. E. Guillet, Macromolecules **27**, 5487 (1994).
- ³⁰J. F. Rabek, *Mechanisms of Photophysical Processes and Photochemical Reactions in Polymers: Theory and Applications* (Wiley, Chichester, 1987).
- ³¹Alternatively, the estimation is based on the measurement of the number of laser pulses necessary for the complete photolysis of ArI within PMMA upon irradiation at low laser fluences (50–100 mJ/cm²). The main error in the approach is introduced by the changes in the substrate absorptivity (due to both Ar-deriving photoproducts and PMMA decomposition products) that are induced in parallel (thus, condition of optically thin sample is not satisfied after extensive irradiation).
- ³²S. Lazare and V. Granier, J. Appl. Phys. **63**, 2110 (1988).
- ³³H. Fujiwara, H. Fukumura, and H. Masuhara, J. Phys. Chem. **99**, 11844 (1995), and references therein.
- ³⁴H. Furutani, H. Fukumura, and H. Masuhara, J. Phys. Chem. **100**, 6871 (1996).
- ³⁵M. N. Ediger and G. H. Pettit, J. Appl. Phys. **71**, 3510 (1992); G. W. Pettit, M. N. Ediger, D. W. Hahn, B. E. Brinson, and R. Sauerbrey, Appl. Phys. A **58**, 573 (1994).
- ³⁶*Handbook of Organic Photochemistry*, edited by J. C. Scaiano (CRC, Boca Raton, FL, 1989), Vol. II; J. C. Scaiano and L. C. Stewart, J. Appl. Phys. **105**, 3609 (1983).
- ³⁷D. P. Brunco, M. O. Thompson, C. E. Otis, and P. M. Doodwin, J. Appl. Phys. **72**, 4344 (1992); S. R. Cain, F. C. Burns, and C. E. Otis, *ibid.* **71**, 4107 (1992).
- ³⁸S. V. Babu, G. C. Couto, and F. D. Egitto, J. Appl. Phys. **72**, 692 (1992).
- ³⁹G. Bounos, A. Athanassiou, D. Anglos, and S. Georgiou (unpublished).
- ⁴⁰S. Chen, I.-Y. S. Lee, W. A. Tolbert, X. Wen, and D. D. Dlott, J. Phys. Chem. **96**, 7178 (1992); I.-Y. S. Lee, X. Wen, W. A. Tolbert, D. D. Dlott, M. Duxtader, and D. R. Arnold, J. Appl. Phys. **72**, 2440 (1992).
- ⁴¹In fact, for weakly absorbing systems, a nonzero slope in the F_{laser} dependence, indicating deviations from this simple formula, is observed even above the threshold. However, because of the previously noted influence of scattering effects on the probing step, we refrain from assigning particular significance to the observed small slopes.
- ⁴²Y. G. Yingling and B. J. Garrison, Nucl. Instrum. Methods Phys. Res. B **203**, 188 (2003).
- ⁴³R. N. Haward and R. J. Young, *The Physics of Glassy Polymers* (Champan and Hall, London, 1997).
- ⁴⁴D. W. van Krevelen and P. J. Hoftyzer, Angew. Makromol. Chem. **52**, 101 (1976).
- ⁴⁵M. L. Williams, R. F. Landel, and J. D. Ferry, J. Am. Chem. Soc. **77**, 3701 (1955).
- ⁴⁶F. Beinhorn, J. Ihlemann, K. Luther, and J. Troe, Appl. Phys. A **68**, 709 (1999).
- ⁴⁷V. N. Tokarev and A. F. H. Kaplan, J. Appl. Phys. **86**, 2836 (1999).
- ⁴⁸F. Weisbuch, V. N. Tokarev, S. Lazare, and D. Debarre, Appl. Phys. A **76**, 613 (2003).